Optimisation of the Sekwa Blended-Wing-Body Research UAV

B.A. Broughton and R. Heise
Council for Scientific and Industrial Research
Pretoria, South Africa

ABSTRACT

A variable stability, blended-wing-body research mini-UAV was developed at the CSIR in South Africa. The purpose of the UAV was to study some of the aerodynamic design and control issues associated with flying wing geometries and to develop a practical methodology for aerodynamic optimisation of this class of UAV. Optimisation was performed in two phases – first optimisation of the planform shape and then the design of a family of optimised aerofoils. The approach was shown to be practical and gave interesting insight into the advantages and challenges of relaxing some of the flying qualities constraints during the aerodynamic design process.

NOMENCLATURE

α_{0L}	zero-lift angle of attack
AoA	α, angle of attack
AR	aspect ratio
BWB	blended-wing-body
$C_{D,0}$	zero-lift drag coefficient
$C_{D,i}$	induced drag coefficient
$C_{D,t}$	total drag coefficient
$C_{m,0}$	zero-lift pitching moment coefficient
CG	centre of gravity
F	objective function to be minimised
S_{actual}	actual wing area
S	reference wing area, as projected into xy-plane

1.0 INTRODUCTION

The Council for Scientific and Industrial Research (CSIR) and Stellenbosch University initiated a research project to investigate and demonstrate several challenges related to flying wing and blended-wing-body configurations. The main objective was to investigate the advantages and pitfalls of using relaxed stability on a blended-wing-body UAV. The project was also aimed at expanding the current aerodynamic and multi disciplinary optimisation capabilities at the CSIR. The project resulted in a mini-UAV incorporating a variable stability control system which is currently undergoing flight testing and which will be used as a research vehicle and technology demonstrator.

This paper discusses the use of mathematical optimisation during the design process. Optimisation was used in two stages:

1. Planform design: After establishing the initial design constraints, mathematical optimisation was used in order to define a planform and to establish the design constraints for the aerofoils.
2. Aerofoils: Once a suitable planform had been selected, a family of eight aerofoils was designed, again using mathematical optimisation.

A separate paper discusses the overall project goals, design process and flight testing of the UAV.

2.0 INITIAL DESIGN

During the initial design phase, overall design constraints such as mass, wing span and wing area were established. These parameters were limited by practical considerations: It was a requirement that the UAV fit into both the low-speed and 7m wind tunnels at the CSIR, effectively limiting the wing span to 1.7m. Design mass was 3.2kg, cruise speed 65km/h and a maximum stall speed of 43km/h was required. These values were similar to those of an existing mini-UAV in the same class that was developed earlier at the CSIR, which would make it an ideal baseline for comparison to the blended-wing-body airframe.

The UAV was to be electrically powered and have endurance in excess of 1 hour. A custom control system would be developed by the Electronics Systems Laboratory (ESL) at the Stellenbosch University. It was initially decided that the natural longitudinal stability of the airframe could be relaxed, to be replaced by a digital artificial stability augmentation system. In order to minimise risk and the amount of time required to develop a custom control system, it was also decided that the airframe had to display good natural lateral flying qualities. This constraint had to be relaxed later in the project for reasons to be discussed in Section 4.0.

The choice of a blended-wing-body was made based on the goals and requirements of the project. No studies were performed to compare this configuration to equivalent conventional layouts, as this is already covered extensively in the literature, albeit less so for airframes of this particular size.

3.0 PLANFORM OPTIMISATION

3.1 Methodology

An overview of the optimisation process is shown in Figure 1. The planform optimisation was done with the principal objective of minimising the induced drag. Although low induced drag was the main objective, it was important to account for the fact that vertical surfaces such as winglets would increase the wetted area without affecting the projected reference wing area. If overlooked, the optimiser would tend to create geometries with very large winglets. One possible solution was to use an analysis program that would look up pre-calculated aerofoil characteristics and then integrate those along the span. This approach would also automatically account for local Reynolds number effects which could be significant at this scale. Although this approach would still not account for 3D viscous effects, such as separation or transition triggered by spanwise flow, it is a viable approach and has been used in other studies, most notably those by Liebeck et al.[1, 2]

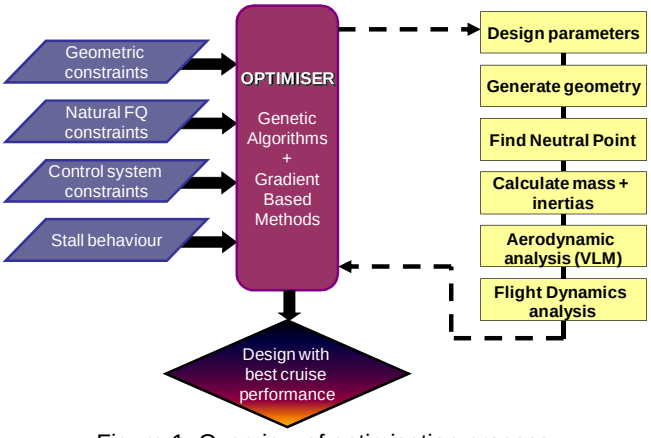

Figure 1. Overview of optimisation process

The only design variables relating to aerofoil shape used in the current wing optimisation problem was local aerofoil camber and pitching moment coefficients. In order to use the table lookup approach described above, more information would be needed about each spanwise section, including the local thickness and aerofoil shape, since the local drag coefficient would be equally sensitive to these parameters as they would be to the camber and pitching moment coefficients already included. The result would have been a large number of design variables, possibly requiring real-time aerofoil analysis rather than table lookups to account for all of them. Instead, it was decided to simplify the drag calculation considerably for the wing optimisation problem, and then to refine each aerofoil separately in phase two of the optimisation, to be described in Section 4.0.

The objective function used in this phase of the design consisted of a constant zero-lift drag coefficient, adjusted for the actual area, and a more detailed induced drag coefficient estimated using a vortex lattice analysis. The objective function to be minimised can be expressed as:

$$F = C_{D,t} = \frac{S_{\text{actual}}}{S} C_{D,0} + C_{D,i}$$

Where S_{actual} is the actual area consisting of the sum of each wing panel in the plane of that panel, S is the wing reference area (the area projected into the xy-plane), $C_{D,0}$ is an estimated zero-lift drag coefficient typical for this type and size of configuration and $C_{D,i}$ is the inviscid induced drag (vortex drag) as estimated by the vortex lattice program. The vortex lattice program used for the analysis was AVL[3].

During the optimisation process, the projected wing area and total mass was kept constant and equal to the values selected during the initial design process. It was, however, necessary to develop a fairly detailed structural mass model in order to account for changes to the moments and products of inertia as the planform shape evolved. The inertias were required for the flying qualities calculations. The outer wing mass model consisted of a beam to represent the carbon fibre main spar caps and foam shear web, while most of the remaining mass was concentrated in the skin, which was built out of a fibreglass and balsa sandwich on the final model. In order to estimate the skin mass and inertias, an approximate aerofoil shape and thickness had to be estimated for each spanwise station. To the basic estimated structural mass and inertias was added mass and inertias due to various avionics components as well as additional structure for the landing gear, motor mount and avionics mounting frame. Some of these components had to be placed based on the current geometry, requiring parametric relations between their positions and the geometry. Furthermore, an additional "moving ballast" was added for each candidate design to bring the total mass up to the target total mass of 3.2 kg. The location of the ballast mass could be adjusted by the design code, which allowed the static margin to be used as a design variable. Finally, a series of checks were included as constraints to the optimisation problem to ensure that each candidate design would be physically realisable from a centre of mass and component placement point of view. As an example, a candidate design that required the ballast mass and some of the components to be placed outside the physical airframe in order to balance the aircraft at the required position would be flagged as unfeasible.

Most of the additional constraints were flying qualities related. Selecting acceptable constraints for the flying qualities can be difficult, since much less work has been done on acceptable UAV flying qualities compared with those for manned aircraft. It was envisaged that some of the test flying would be done manually, using the control system as a stability augmentation system when required. In general, it was found that flying qualities required for human-in-the-loop flying tended to be stricter than those for fully automated flight. As an initial starting point, Mil-STD-8785C was used as a basic guideline for quantitative values required for acceptable flying qualities, with some adjustments to be discussed later. In the case of longitudinal flying qualities, it was accepted that the control system would be used as a full authority augmentation system, allowing considerable relaxation of the natural flying qualities constraints. Even with stability augmentation, some limitations still had to be observed – the slew rates available from the servos, practical control surface sizes and the processor speed as well as the digital sampling rates all placed limitations on the practical allowable level of instability. It was found, however, that only a small amount of instability was required for maximum efficiency during cruise so that these constraints were seldom active during the optimisation process. The flying qualities constraints are summarised below:

- The real component of any unstable root had to be less than 1 rad/s
- If unstable, the spiral mode had to have a time-to-double of more than 12 sec.
- The roll mode time constant had to be less than 1 sec.
- The dutch roll natural frequency had to be greater than 1 rad/s.
- The dutch roll damping ratio had to be more than 0.4. This constraint was later reduced to 0.1 (see Section 3.2)

Since the UAV would be flown manually during some of the flight testing, it was important that stall characteristics be controllable. To reduce the likelihood of a tip-stall tendency, a constraint was added that required the local lift coefficient near the wingtip (over the last 10% of the semi-span) to be less than 80% of the maximum local lift coefficient over the inner 50% of the wing. This constraint was enforced at a total lift coefficient of $C_L = 1.1$.

It was also required that the elevons be faired (less than 1 degree positive or negative deflection) during flight. At the same time, aerofoils were required to have conventional negative pitching moments (no reflex) in order to meet the maximum lift coefficient constraint. In the past, one way to trim flying wings was to use highly swept planforms with download towards the tips for trim at positive static margins. This destroys the optimal lift distribution, however, so that the aircraft had to pay a penalty both in the form of induced drag and a reduced overall maximum lift coefficient. By allowing the slightly negative static margin, all the constraints listed here could be met while still employing a close to optimal lift distribution.

The geometry was parameterised by dividing it into five spanwise panels, each of which could be described by its own sweep angle, taper ratio, dihedral angle and twist angle. A typical planform is shown in Figure 2. At the root and tip of each panel, the local section pitching moment coefficient ($C_{m,0}$) and zero-lift AoA (α_{0L}) could be specified. This required a "dummy aerofoil" to be designed at each of these stations as the design evolved, in order to generate the shape of the camber line required for the vortex lattice analysis. An inverse aerofoil design program called PROFOIL[4,5] was used to generate these shapes. As described before, the final design parameter was the static margin.

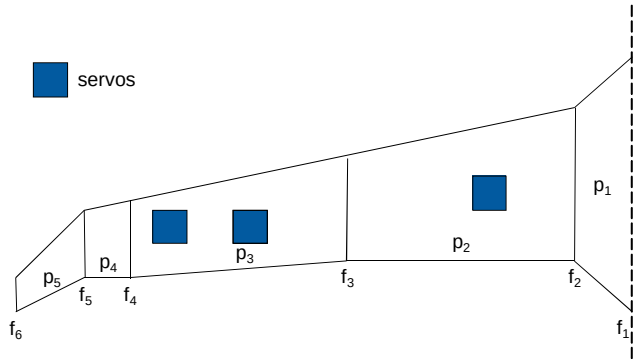

Figure 2. Planform parameterisation

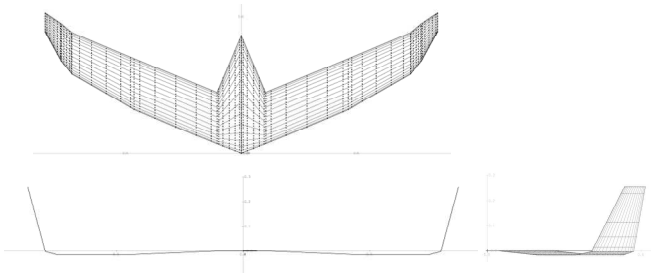

Figure 3. Vortex lattice model of final design

It was stated before that the wing reference area (the projection of the wing planform in the xy-plane) was selected during the initial design phase and maintained as a constant during the optimisation process. In order to do this, one of the geometric design parameters had to be given up. The one selected was the taper ratio of the inner fuselage panel. The relative spanwise lengths of all the panels were selected before the optimisation process started, and the total length scaled to match the prescribed wing span of 1.7m.

Induced drag, stability and control derivatives were predicted using the vortex-lattice code AVL. A custom C++ code was developed for generating the geometry and estimating the mass and inertia values of the structure and avionics systems. Another custom code was used to predict the flying qualities and controllability of each candidate design. Part of this analysis consisted of using the eigenvectors to automatically identify each mode and its corresponding eigenvalues. A commercial optimisation package was used, providing a combination of genetic algorithms and gradient based methods. Due to the very fast analysis time, it was possible to perform the optimisation process using a genetic algorithm. Once the genetic algorithm converged on a feasible design, a gradient based method was used to refine the design and to perform sensitivity studies.

3.2 Results

A three-view diagram of the final vortex lattice model is shown in Figure 3. The static margin selected by the optimiser for the final design was close to zero, despite the strict negative pitching moment constraints enforced by the design. The control system was capable of handling significantly more negative static margins. The sweep of the wing was mostly driven by lateral flying qualities constraints, but it is this sweep that also made trimming the aircraft possible without reverting to low pitching moment aerofoils. In future studies, it may be interesting to also relax some of the lateral flying qualities constraints and compare the results to the current design.

The spanwise load distributions are shown in Figures 4 and 5 for the trimmed cruise and near stall conditions respectively. Although the complex wing geometry and the presence of the fuselage make the ideal elliptical lift distribution unlikely to be achieved, the spanwise efficiency was quite high due to the presence of the winglets. The efficiency factor was, in fact, approximately 1.1 during the cruise condition. The near stall condition shows that the local lift coefficient gradually decreases towards the tip, despite the small chord of the winglet. Although the possibility of a tip-stall

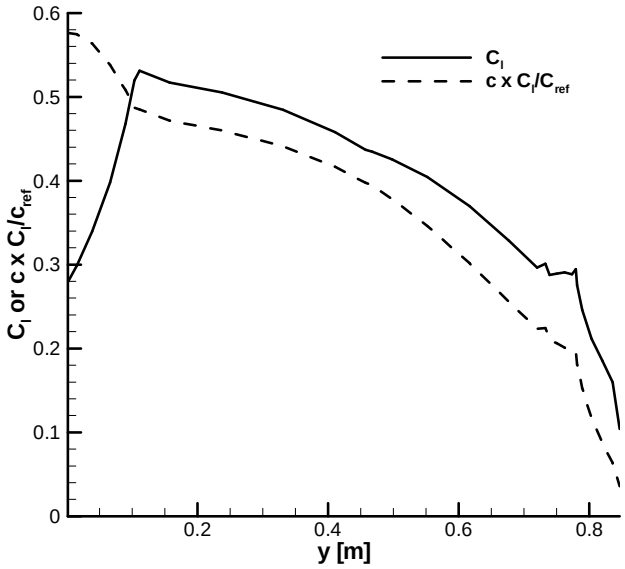

Figure 4. Trimmed spanwise load distribution in cruise

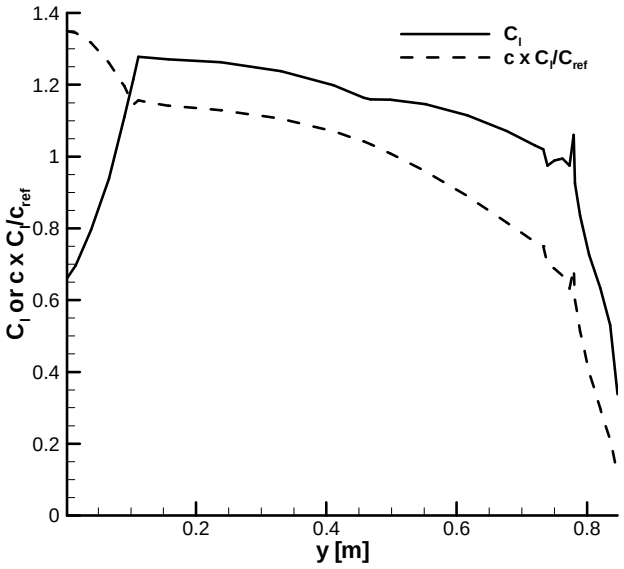

Figure 5. Trimmed spanwise load distribution close to stall

tendency still exists, especially due to the presence of all the control surfaces, this lift distribution should limit this tendency.

Since the centre of mass was adjustable in flight, the interesting option exists to shift the CG backwards for the landing configuration resulting in a nominal down elevon position. Analysis of the final design showed that this would be quite possible with negative static margins well within the capabilities of the control system. Although it would not quite be possible to have the full effect that flaps would have given on a conventional design, the relaxed stability does mean that sizing a flying wing for take-off and landing performance will not result in the oversized wing often required for flying wing designs.

As mentioned in Section 2.0, the dutch roll damping ratio constraint was relaxed from 0.4 to 0.1 as the design developed. The value of 0.4 was selected based on recommendations in Mil-STD-8785C. It was, however, quickly discovered that this constraint tended to drive the entire design. It resulted in very large winglets, which in turn came with a large wetted area penalty. Instead, the constraint was relaxed to 0.1 (at which point it was not active anymore at the final design). This low damping ratio would be unacceptable for manned aircraft. On UAVs, the suitability of a flying quality constraint such as this one is less clear. Model aeroplanes are often flown with flying qualities that would be unacceptable for manned aircraft, without any complaints from the pilot. On the other hand, a lightly damped dutch roll mode would

be less than ideal for a camera platform, especially on small UAVs where the payloads are often not stabilised or only stabilised about one axis. It was therefore decided to implement a yaw damper in the control system to increase the dutch roll damping. This was easily implemented by utilising the rudders on the winglets as control effectors.

It should be noted that the vortex lattice model is a simplified, idealised geometry. A disadvantage of the vortex lattice approach is that subtle details in the geometry may not be captured by the analysis method. As follow-on work to the current project a fast parametric mesh generator was developed that would allow replacing the vortex lattice method with a panel method. The new code can generate fairly complex curved wing panels, which should in future lead to considerably more refined designs at this early stage of the optimisation process.

4.0 AEROFOIL OPTIMISATION

4.1 Introduction

Over the years, many papers have appeared in the literature on aerofoil optimisation and a multitude of methodologies exist, each with its own advantages and disadvantages. In selecting a method for the current project, the goals were principally flexibility in specifying a fairly large number of design constraints and robustness. Computational efficiency was of secondary importance, although follow-up work is underway to improve the efficiency of the algorithms for future applications.

As explained in the introduction to this paper, the optimisation process of the airframe was simplified somewhat by dividing it into two distinct stages, namely planform and aerofoil optimisation. Some of the results of the planform optimisation were needed as aerofoil design constraints, so it was important to ensure that the planform design could be frozen before continuing with the aerofoil design process.

The reader will notice that the authors used an inverse aerodynamic design tool for the aerofoil optimisation. An experienced designer can often design very efficient aerofoils without the use of mathematical optimisation when utilising such a tool combined with a more detailed analysis method. Even when using the tool as part of an optimisation method, the authors performed some manual studies to determine the most efficient ways in which to parameterise and analyse the aerofoils. Only once a good understanding of the parameters involved was obtained, did the authors switch to optimisation. Once again, thorough sensitivity studies were performed when any constraint was active, or when any uncertainty over the selection of a constraint existed.

4.2 Methodology

The optimisation consisted of multipoint optimisation to give a slightly wider useable operating range than that which would result when optimising for a single flight condition. For each aerofoil, the vortex lattice model was used to extract the local lift coefficient when the aircraft was at three different flight conditions, namely cruise, a lower "loitering speed" and the maximum speed. The objective function was composed of the computed drag coefficients under each of these operating conditions:

$$F = 3C_d|_{\text{cruise}} + C_d|_{\text{max speed}} + C_d|_{\text{loiter}}$$

Note that the cruise drag coefficient was weighted heavier than the drag coefficients calculated at the other two operating conditions. For each flight condition, the local Reynolds number and lift coefficient were used when calculating drag. The XFOIL[6] aerofoil analysis code was used for all viscous drag calculations.

Two additional constraints were added:

- Maximum lift coefficient: The vortex lattice analysis was used to find the local lift coefficient required at a given spanwise location when the wing was trimmed for the target stall speed condition. The aerofoil at this location was then required to have a maximum lift coefficient higher than that computed from the vortex lattice analysis.
- A geometric volume constraint, usually in the form of a box with a given location, width and depth, was added based on the local requirement. At the centre "fuselage" station, the size of this box was determined by the physical dimensions of the avionics, while spar depth typically determined the limits on the wing and winglet stations.

The aerofoil pitching moment coefficient ($C_{m,0}$) and zero-lift AoA (α_{0L}) were constrained to the values computed during the planform optimisation process. Normally these would also be added as aerodynamic constraints to be satisfied during the optimisation process, but by using an inverse design code for generating aerofoil geometries, the requirement could automatically be satisfied by each candidate aerofoil without having to constrain them as part of the optimisation process.

The aerofoils were parameterised using the input to the PROFOIL[4,5] aerofoil design code. PROFOIL is an inverse design code developed at the University of Illinois. It allows the user to prescribe the velocity distribution over the aerofoil at various operating conditions, and also allows the user to specify additional geometric or aerodynamic constraints including the pitching moment coefficient, zero-lift angle of attack, maximum thickness and trailing edge thickness – all of which were prescribed in the current study. The maximum thickness was actually applied as one of the design parameters. An alternative to the inverse design approach is to use a geometric parameterisation of the aerofoil. Several such parameterisations exist – from simple ones controlling camber, location of maximum camber and other "global" geometric parameters, to ones that physically move a large number of nodes on the surface of the aerofoil. Another approach is to use parametric splines such as NURBS to describe the aerofoil shape. All these methods have been used successfully by various groups. The current approach has the advantage that some of the constraints, even aerodynamic constraints, could be satisfied automatically by each candidate design. The main design parameter becomes the shape of the pressure distribution, which is very closely related to the boundary layer development, which in turn is the reason why excellent aerofoils can be designed using inverse design methods even without the use of optimisation. A list of design variables are given below:

- 14 variables controlling the shape of the pressure distribution. This number was increased to 30 as each design was refined in stages. Over some portions of the aerofoil, the shape of the pressure distribution was not specified up front in order to allow the inverse code to satisfy other constraints.
- The trailing edge angle (angle between the upper and lower surface gradients at the trailing edge).
- Three parameters used by the inverse code that influence the velocities near the trailing edge.
- Maximum thickness ratio of the aerofoil

The following characteristics were directly enforced through the inverse code. It should be noted that aerodynamic characteristics refer to inviscid characteristics, which may in some cases be slightly violated in the viscous analysis:

- Pitching moment coefficient ($C_{m,0}$).
- Zero-lift angle of attack (α_{0L}).
- Trailing edge thickness. This was specified as 0.8mm over the entire span of the wing, which resulted in a fairly thick ratio towards the tip of the winglet where the chord became quite narrow.

Analysis of the candidate aerofoil was done using XFOIL. Special attention had to be given to the maximum lift coefficient constraint: XFOIL allows the user to perform an analysis either at a specified angle of attack, or a specified lift coefficient. Determining the drag

Table 1
List of aerofoil sections

Section #	Description
1	Centre of fuselage
2	Fuselage station at y=50mm
3	Middle of fuselage/wing fairing
4	Root of inner wing panel
5	Transition from inner to second panel
6	Tip of second wing panel
7	Root of winglet

coefficient at each operating condition therefore only required one solution at each lift coefficient. Maximum lift coefficient, on the other hand, would require a series of solutions at various angles of attack, after which the maximum lift coefficient would have to be determined either through an iterative process or estimated through a curve fit. This one constraint would therefore require the majority of the computational time, even though the wide drag bucket meant it was seldom active near the optimum aerofoil shape. Instead of this computationally intensive approach, an alternative method was used where a simple test was performed: XFOIL was used to perform a computation at the value of the maximum lift coefficient constraint. If XFOIL converged, the constraint was satisfied and no further computations were required. If the constraint was not satisfied, that particular design was heavily penalised. This approach could only be used when using a genetic algorithm for the optimisation process, since it would be impossible to calculate a penalty function gradient using this approach.

The optimisation was performed in three stages of increasing resolution over the specified velocity distribution. During the first stage, the genetic algorithm was used which resulted in a feasible design close to the optimum shape. Although computationally expensive due to the thousands of function evaluations required, it did make it likely that a global minimum would be found. Conveniently, it was found that the maximum lift constraint was inactive near the optimum design of all the aerofoils. The first and second refinement could therefore use a gradient based method from a commercial optimisation package, each time starting with the best design from the previous stage.

A family of eight aerofoils were designed for the entire UAV, with the intermediate spanwise sections using geometric interpolations between them. The aerofoil positions are described in Table 1.

4.3 Results

Two of the aerofoils driven by different constraints will be discussed here. The first is the root aerofoil at the centre of the fuselage. This particular aerofoil had to house the avionics box. Enough space was required to allow the box to slide forwards and backwards to change the CG in flight as commanded by the variable stability system. This volume required a fairly thick aerofoil, although this thickness was one of the design variables and the optimisation program was allowed to adjust the shape and thickness of the aerofoil via the inverse input as required to fair in the avionics box. The final aerofoil shape is shown in Figure 6, with the location of the avionics box indicated as the dashed rectangle. It can be seen the optimisation program fitted the aerofoil closely around the corners of the avionics box, although it doesn't actually touch the rear corners.

Figure 7 shows the pressure distribution corresponding to this aerofoil at the cruise condition as computed with XFOIL. There is a noticeable "bump" near the leading edge as the optimiser attempted to fit the avionics tray into the aerofoil in this region. Also notice that the flow was still attached at the trailing edge after encountering only a small laminar separation bubble on the upper surface, despite the thick section and relatively low Reynolds number. Meeting all the constraints for this aerofoil while still minimising drag would be difficult without the use of mathematical optimisation. The objective function value and the separate drag

Table 2
Optimisation results for fuselage centre aerofoil

	Initial	Final
$C_{l,max\ speed}$	0.18	0.18
$C_{d,max\ speed}$	0.011119	0.006747
$C_{l,cruise}$	0.30	0.30
$C_{d,cruise}$	0.012963	0.007107
$C_{l,loiter}$	0.50	0.50
$C_{d,loiter}$	0.015424	0.008820
F	0.065431	0.036889
Box depth	0.078367	0.077457
$C_{l,stall}$	ok	ok

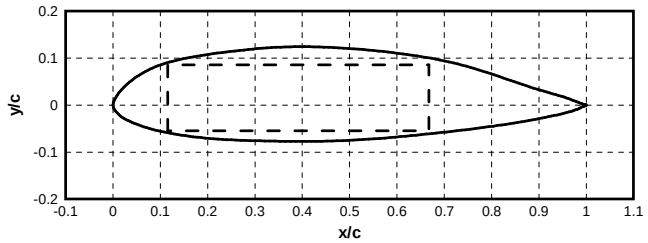

Figure 6. Root aerofoil with avionics box volume

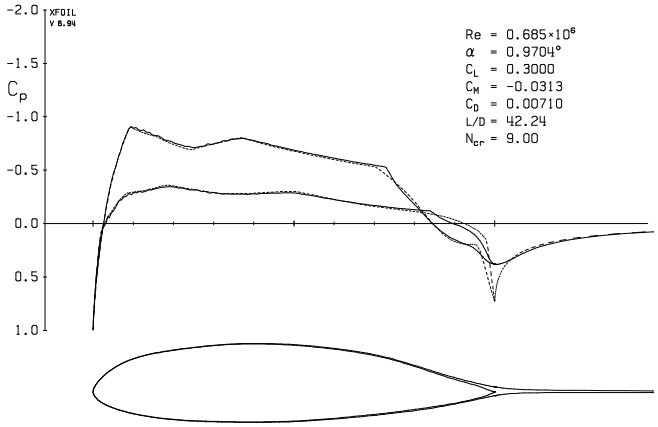

Figure 7. Pressure distribution over optimised root aerofoil

values are listed in Table 2 for an initial design and the final optimised design. The objective function value was reduced with 44%. In the experience of the author, this magnitude of improvement is not uncommon for low Reynolds number aerofoils where the pressure drag due to separation bubbles or early separation can often be drastically reduced.

The pressure distribution over the optimised aerofoil at the transition from the inner to outer wing panel (approximately halfway along the span) is shown in Figure 8. The results of the optimisation process for the initial and final designs are listed in Table 3. The initial design used for this aerofoil was taken from the aerofoil for the previous section, so that it was already close to optimised. Despite the good initial aerofoil shape estimate, the objective function value was still reduced with 16% from the initial to the final design.

The results shown for the two aerofoils here are representative of all eight aerofoils designed for the UAV. It was found that convergence of the analysis routine became slower during the design of the outer aerofoils. The reasons for this were two-fold: First, the Reynolds number became quite small towards the tip of the wing and second, the relative thickness of the trailing edge became very thick in order to maintain the absolute trailing edge thickness of 0.8 mm (selected due to a manufacturability limitation). The total optimisation process would take a few days for each aerofoil, as manual interaction was required as the parameterisation was refined between optimisation stages. The

Table 3
Optimisation results mid-span aerofoil

	Initial	Final
$C_{l,max\ speed}$	0.26	0.26
$C_{d,max\ speed}$	0.014511	0.011532
$C_{l,cruise}$	0.50	0.50
$C_{d,cruise}$	0.011297	0.009419
$C_{l,loiter}$	0.70	0.70
$C_{d,loiter}$	0.012188	0.011278
F	0.060590	0.051067
$C_{l,stall}$	ok	ok

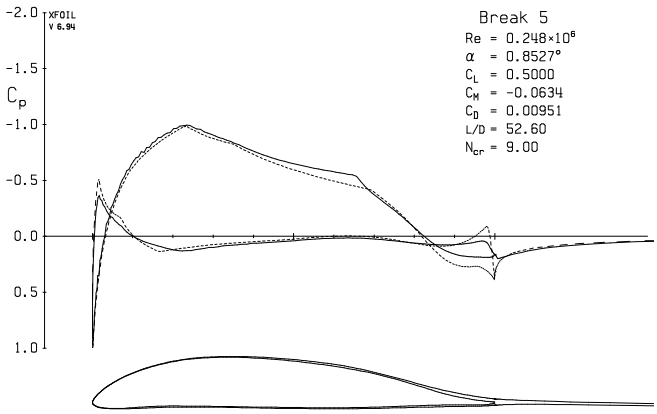

Figure 8. Pressure distribution over mid-span aerofoil

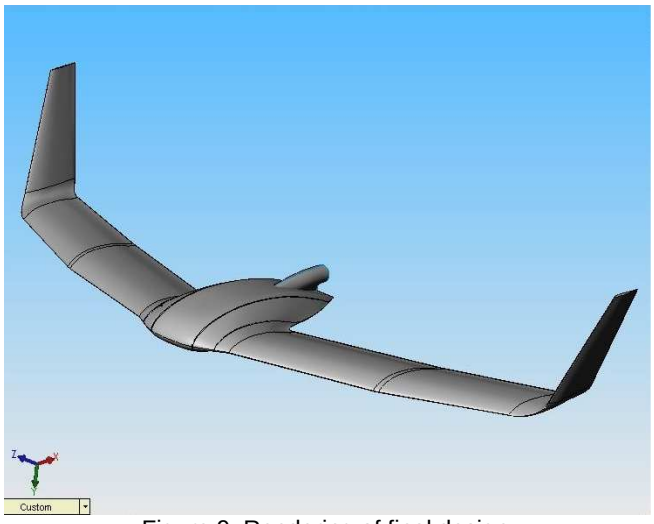

Figure 9. Rendering of final design

most time-consuming was the initial genetic algorithm design stage, which could take up to a day or more. The final CAD geometry, after assembling all the aerofoils and smoothing the panel transitions, is shown in Figure 9.

5.0 CONCLUSIONS

Mathematical optimisation was used during the aerodynamic design of the Sekwa blended-wing-body research UAV. The optimisation process was very effective, although time consuming and it occasionally required manual intervention due to failure of the analysis methods to converge. The correct selection and application of the optimisation constraints need to be done carefully, especially during the planform optimisation process, as they can have a large influence on the final design. Future studies may in particular look at the advantages associated with relaxing some of the lateral flying qualities constraints. Based on experience gained on this project, a set of custom optimisation algorithms are being developed for the aerofoil optimisation process to deal more effectively with the occasional failure of the analysis method. A new parameterised mesh generator has also been developed that will allow the use of a panel method earlier in the design process, possibly replacing much of the vortex lattice work. The approach of performing the optimisation process in two stages was effective, although the ultimate goal is still to perform the complete three dimensional shape optimisation in a single optimisation methodology.

REFERENCES

1. ROMAN, D., ALLEN, J.B. AND LIEBECK, R.H. Aerodynamic Design of the Blended-Wing-Body Subsonic Transport, August 2000, AIAA Paper 2000-4335.
2. LIEBECK, R.H. Design of the Blended-Wing-Body Subsonic Transport, January 2002, AIAA Paper 2002-0002.
3. DRELA, M. AND YOUNGREN, H. AVL 3.26 User Primer, April 2006.
4. SELIG, M.S. AND MAUGHMER, M.D. A Multi-Point Inverse Airfoil Design Method Based on Conformal Mapping, *AIAA Journal*, 1992, **30**, (5), pp 1162-1170.
5. SELIG, M.S. AND MAUGMER, M.D. Generalized Multipoint Inverse Airfoil Design, *AIAA Journal*, 1992, **30**, (11), pp 2618-2625.
6. DRELA, M. XFOIL: An Analysis and Design System for Low Reynolds Number Airfoils, *Low Reynolds Number Aerodynamics*, 1989, **54** Springer-Verlag Lecture Notes in Engineering.